Conference Paper, Published Version

Zhang, Qinghui; Escobar, Sebastian; Toorman, Erik; Monbaliu, Jaak

Two-dimensional computations of Stokes drift and undertow at the near coast region

Zur Verfügung gestellt in Kooperation mit/Provided in Cooperation with:
TELEMAC-MASCARET Core Group

Verfügbar unter/Available at: https://hdl.handle.net/20.500.11970/107449

Vorgeschlagene Zitierweise/Suggested citation:
Zhang, Qinghui; Escobar, Sebastian; Toorman, Erik; Monbaliu, Jaak (2020): Two-dimensional computations of Stokes drift and undertow at the near coast region. In: Breugem, W. Alexander; Frederickx, Lesley; Koutrouveli, Theofano; Chu, Kai; Kulkarni, Rohit; Decrop, Boudewijn (Hg.): Online proceedings of the papers submitted to the 2020 TELEMAC-MASCARET User Conference October 2020. Antwerp: International Marine & Dredging Consultants (IMDC). S. 159-164.

Two-dimensional computations of Stokes drift and undertow at the near coast region

Qinghui Zhang[1],Sebastian Escobar[1], Erik Toorman[1], Jaak Monbaliu[1]
[1] Department of Civil Engineering, KU Leuven
Leuven, Belgium
Qinghui.zhang@kuleuven.be

***Abstract*— Stokes drift is the net transport velocity experienced by water particles in the direction of wave propagation. In offshore regions, it plays a role in the fate and transport of pollutants (e.g. oil spills, plastics, POPs). When it comes to near-coastal regions, Stokes drift transports water mass towards the coastline, generating a return flow close to the bottom due to the no-flow boundary condition imposed by a beach [12]. This return flow, termed as 'undertow', plays an important role for the determination of wave-induced sediment transport and sandbar migration, shaping the ocean bottom close to the coast.**

Under the Eulerian frame, the direct computation of Stokes drift and subsequent undertow is not possible due to their Lagrangian nature. Following the complete Lagrangian transport of individual water parcels, caused by the superimposed effect of waves and currents leads to a very huge, even impossible workload for multi-dimensional turbulent flow solvers. A mixed Eulerian-Lagrangian 'GLM' formalism, which splits the total motion into a mean part and an oscillatory part was proposed [1]. This framework averages on the Lagrangian feature of waves, and the final equations obtained are conveniently written under Eulerian coordinates.

In our work, we have introduced the depth-averaged GLM approach in TELEMAC-2D. The Stokes drift and the subsequent undertow were obtained from a coupled TELEMAC-2D-TOMAWAC calculation. It was shown that for a bottom with a constant slope, the wave energy breaking occurs further to the offshore than in the measurements. The undertow has also been underestimated.

The underlying reason could be attributed to the lack of a roller implementation in TOMAWAC, and the possible interference caused by the deactivation of the bottom friction laws in TELEMAC-2D for all laboratory cases listed in this study. The roller is responsible for partially transporting the wave energy during breaking and gradually releasing it during the surf zone wave propagation. The roller also brings water mass further to the coast, and leads to a larger return flow. This effect has been observed to be less important for a barred bottom and an irregular bathymetry, where the wave breaking occurs in several positions, and the effect of the roller is less significant. The influence of no bottom friction as well as the quadratic bottom friction should be investigated in further studies.

I. Introduction

The interaction between ocean surface gravity waves caused by wind and slowly varying currents in near coastal regions has drawn widespread attention. On one hand, the waves experience dramatic transformations in these regions and exert space- and time-dependent forces on the water body, generating water surface set-up, set-down and alongshore currents. On the other hand, the ambient currents and local water depth impact the propagation and breaking of the waves, exchanging energy with the mean currents. By means of intensive measurements and numerical computations on a rapidly eroding coast, the effects of important wave heights are emphasized in relation to the movements of sediments [12].

In practical applications, the computational cost is significant if the surface variations by short gravitational waves are resolved, a common practice is to use a spectral phase-averaged model for the wave energy propagation and transformation (third generation wind wave model). In the context of a depth-integrated hydrodynamic model, the waves influence the currents momentum distribution by adding an extra momentum flux (forcing) through the form of a divergence of radiation stress. For shoaling zones and wave breaking zones, this generates a set up and set down of the free surface. The formulation is well established in [7]. Waves influence also the mass transport of the water body through a high order phenomenon, Stokes drift. It is the net transport velocity experienced by water particles in the direction of wave propagation. In the near-coastal region, Stokes drift transports water mass towards the coastline, generating a undertow close to the bottom due to the non-flow boundary condition. In order to numerically capture the Stokes drift and undertow in nearshore models, a mixed Eulerian-Lagrangian 'GLM' formalism, which splits the total motion into a mean part and an oscillatory part was proposed [1]. This frame averages on the Lagrangian feature of waves, and final equations obtained are conveniently written under Eulerian coordinates.

The outline of the paper is as follows: the second section is devoted to the GLM formalism and the governing equations written in terms of the Lagrangian velocity in non-conservative forms; in the third section, the simulation of three experimental tests of wave set-up and set-down and return flow, including bathymetries composed of a constant slope, a barred bottom and an irregular topography are discussed; they are followed by the conclusion and future work.

II. GLM FORMALISM, GOVERNING EQUATIONS

A. Stokes drift and undertow

When surface gravity waves travel in water, the leading order of the particle movement caused by waves is periodic, forming from closed ellipses to circles depending on the water depth relative to wavelength. However, higher order mathematical calculations show that after one wave cycle, the particle experiences a net transport forward in the direction of wave propagation. It is a combined effect of particle spending more time in the forward-moving region and undergoing the forward motion at higher water height, where velocities are larger [5]. This higher-order phenomenon, termed as 'Stokes drift', is essential for certain coastal processes such as wave-induced sediment transport and subsequent coast erosion and bar migration close to near coast zone, where the zero flux beach condition imposes a return flow. Figure 1 demonstrates a typical vertical Stokes drift profile for a monochromatic wave. The resulting undertow due to the no-flow land condition is shown in figure 2.

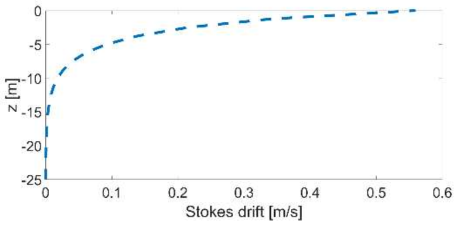

Figure 1 Stokes drift under monochromatic waves, the wave period is 5s and the wave amplitude is 1.5m. The mean water depth is 25m.

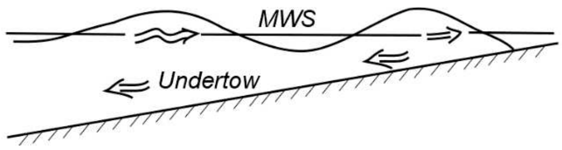

Figure 2 Stokes drift near the surface and undertow close to the bottom. Figure reproduced based on the figure in [4].

B. Governing equations in GLM formalism

In light of considering the wave-induced Stokes drift and subsequent return flow, the shallow water equations in TELEMAC-2D are cast into a depth-averaged GLM formulation in terms of the Lagrangian velocity (u^L and v^L). It is the sum of the averaged Eulerian velocity (u^E and v^E) and the Stokes drift ($\overline{u}^S$ and $\overline{v}^S$). For a full three-dimensional description of the system, readers are referred to [8]. Aiming to be consistent with the TELEMAC system, we write the equation in non-conservative form:

$$\frac{\partial u^L}{\partial y} + g\frac{\partial \eta}{\partial x} = f v^L + \nu_h\left(\frac{\partial^2 u^L}{\partial x^2} + \frac{\partial^2 u^L}{\partial y^2}\right) + \frac{\tau_{sx}}{\rho h} - \frac{\tau_{bx}^E}{\rho h} + \frac{F_x}{\rho h}$$

$$\frac{\partial v^L}{\partial t} + u^L\frac{\partial v^L}{\partial x} + v^L\frac{\partial v^L}{\partial y} + g\frac{\partial \eta}{\partial y} = -f u^L + \nu_h\left(\frac{\partial^2 v^L}{\partial x^2} + \frac{\partial^2 v^L}{\partial y^2}\right) + \frac{\tau_{sy}}{\rho h} - \frac{\tau_{by}^E}{\rho h} + \frac{F_y}{\rho h}$$

Where h is the water depth, η is the free surface level, f is the Coriolis coefficient, ν_h is the horizontal viscosity, τ_{sx} and τ_{sy} are the wind shear stresses, F_x, F_y are wave induced forces τ_{bx}^E and τ_{by}^E are the bed shear stresses. Note that we consider that in reality, the depth-averaged Stokes drift is distributed close to the surface of the flow and thus the bottom shear stress is a function of only the quasi-Eulerian velocity, which in the vicinity of the coast is directed towards the offshore. In TELEMAC-2D, it is computed as follows:

$$\tau_{bx}^E = -\frac{1}{2}\rho C_f u_E\sqrt{u_E^2 + v_E^2}$$

$$\tau_{bx}^E = -\frac{1}{2}\rho C_f v_E\sqrt{u_E^2 + v_E^2}$$

where C_f is a dimensionless friction coefficient. The depth averaged Stokes drift is computed as:

$$(\overline{u}^S, \overline{v}^S) = \frac{\sigma_p \mathbf{k}_p H_s^2}{16 k_p h \tanh(k_p h)}$$

with σ_p and $\mathbf{k}_p$ being the wave's intrinsic angular frequency and wave number of peak wave energy, H_s is the significant wave height and h is the water depth. The wave-driven force, thus the divergence of radiation stress:

$$F_x = -\left(\frac{\partial S_{xx}}{\partial x} + \frac{\partial S_{xy}}{\partial y}\right)$$

$$F_x = -\left(\frac{\partial S_{yx}}{\partial x} + \frac{\partial S_{yy}}{\partial y}\right)$$

where the radiation stress components are given by:

$$S_{xx} = \rho g \int\int [n\cos^2\theta + n - 0.5]E(f,\theta)df\, d\theta$$

$$S_{xy} = \rho g \int\int [n\, sin\theta \cos\theta]E(f,\theta)df\, d\theta$$

$$S_{xx} = \rho g \int\int [n\sin^2\theta + n - 0.5]E(f,\theta)df\, d\theta$$

where n is the ratio between the wave's group velocity and the phase velocity. $E(f,\theta)$ is the spectral density of the surface wave elevation. f is the wave frequency and θ is the wave's propagation direction.

The two-way coupling of TELEMAC-2D and TOMAWAC is achieved in the following manner: TELEMAC-2D provides water depth and Lagrangian currents to TOMAWAC for the wave action conservation equation. Stokes drift and wave driven force are computed in TOMAWAC with wave parameters, and they are passed into TELEMAC-2D. The former provides extra mass transport together with the mean current, and the latter brings an added momentum flux into the force balance of currents. The effects of the coupling will be validated in the following theoretical tests, where the stationary wave shoaling and breaking exert space varying forces on currents, leading to a new equilibrium water level with set-up and set-down. Moreover, the undertow in these tests have been measured and compared to the numerical simulations.

III. VALIDATION OF TELEMAC-2D-TOMAWAC IN THE GLM FORMALISM: WAVE SHOALING & BREAKING

The developed 2D averaged wave current interaction model has been validated with laboratory tests. The first test case consists of a laboratory test for which the bottom topography presents a constant slope. The test case has been presented in [11], with the undertow velocity measured by an Argon-Ion

Laser Doppler Velocimeter. The length of the test domain is 25m, and the width is 10m. At the lateral horizontal boundaries, a zero-gradient free surface boundary condition has been imposed. A fixed 0m free surface has been imposed at the offshore boundary, which leads to a water depth of 0.46 meters. The bathymetry has a constant slope of 1/35 therefore the bottom meets the surface level of 0m at 16.1m length (see figure 3).

A steady TMA spectrum is imposed at the offshore boundary, with a significant wave height of 0.0829m, and a peak period of 1.5s. The main direction of the waves is perpendicular to the coast, with a boundary directional spread of 1500, thus leading to a very narrow angular distribution function (see figure 4).

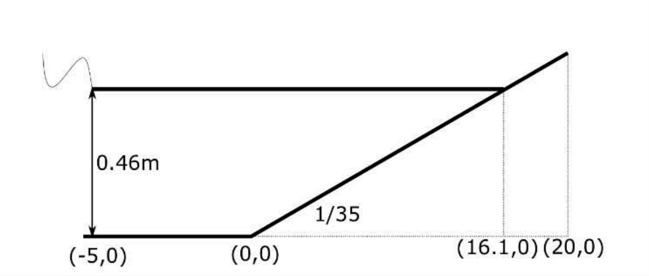

Figure 3 Bottom configuration for the test case of constant slope.

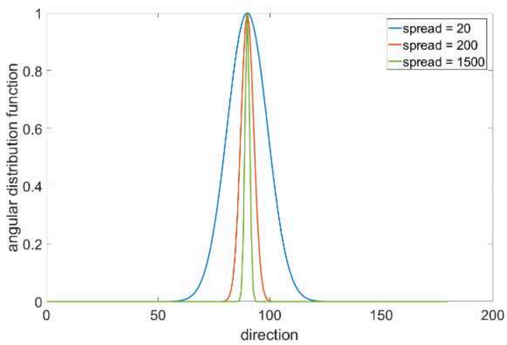

Figure 4 Angular distribution function for computing the boundary spectrum as a function of the directional spreading.

From a zero surface initial condition, the wave driving forces generate a velocity that transports water mass, and slowly brings the surface to an equilibrium state, balancing the radiation stress gradient in the cross-shore direction. The computed wave height, free surface (wave set-up, set-down) and undertow have been compared to the measurements (see figure 5). The wave height (wave energy) demonstrates a slight delay compared to the measurements. The free surface wave set-up has been well captured, except for the very shallow part. It could be related to the application of a numerical clipper in TELEMAC-2D to avoid negative water depth (for water depths less than 5cm). The undertow has been well captured at the deep part, but in the shallower zone it is underestimated. Both the undertow and delay of wave breaking could be caused by lack of a roller, which is a phenomenon that stores the wave energy and brings an extra mass of water to the coast. This is further testified by conducting a second test case, where the bottom is composed of a barred beach, leading to an extended wave breaking, which occurs in several positions.

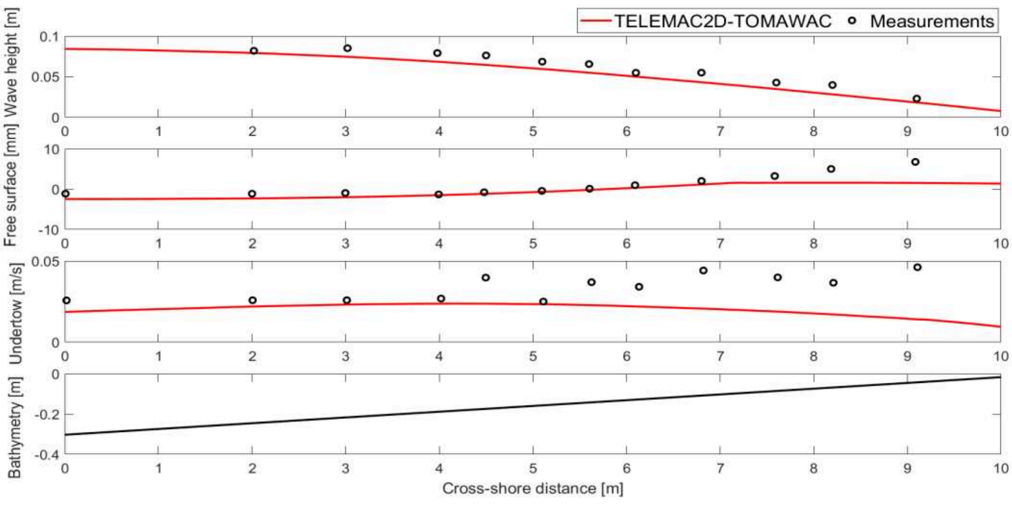

Figure 5 Simulate wave height, free surface and undertow have been compared to the measurements presented in [11].

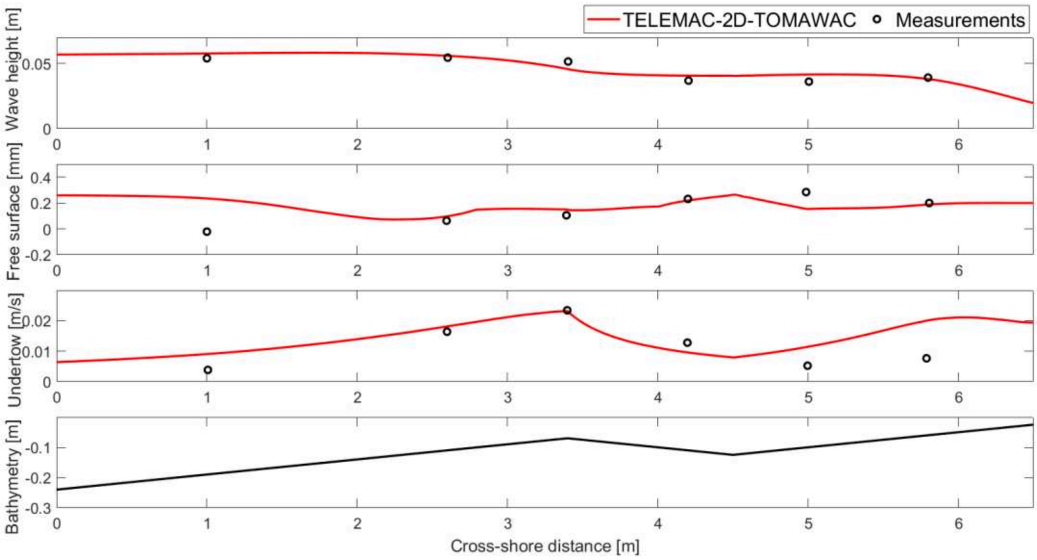

Figure 6 Simulate wave height, free surface and undertow have been compared to the measurements for the barred test case presented in [9].

The laboratory barred test case was presented in [9]. It is a one-dimensional case, with a length of 17m and a width of 2m. Similar to the previous case of the constant slope, at lateral boundaries a zero-gradient free-surface level was applied. The water depth at the offshore is 0.32m, where a Bretschneider-Mitsuyasu spectrum was imposed, with a rooted-mean-squared wave height of 0.0397m and a peak period of 0.945s. Other settings are identical to the previous case. The comparison between the computed quantities and the measurements is shown in figure 6. Compared to the case of a constant slope, the wave breaking occurs at two locations where the water depth decreases, with a slight wave shoaling in between. The wave height variation along the propagation is better captured, yielding also a satisfying free surface variation. The undertow variation and its magnitude are better simulated as well, with no systematic underestimation observed as for the previous test case.

The third case demonstrates to be a prototype of a large field campaign (DUCK 94 field experiment [6]). It has been presented in [10]. The model length is 110m long and 40m wide. The water depth at the left boundary is 4.6m, where a TMA spectrum with a wave height of 0.5 m and a peak period of 4s has been imposed. The irregular bottom profile has been obtained by approximating the bar geometry for the average profile observed of the DUCK94 campaign at a 1:3 scale. The undertow velocity measurements have been obtained with an Acoustic Doppler Velocimeter. The numerical simulation results have been compared to the measurements, and it is shown in figure 7.
The wave breaking has been well captured. In terms of the free surface, the set-down has been underestimated, which could be related to the imposed water depth boundary condition at the offshore. The overall undertow profile has been well reproduced as well, compared to the case of the constant slope.

IV. CONCLUSIONS AND FUTURE WORK

In this study, the Stokes drift and undertow computation have been implemented in the TELEMAC-2D-TOMAWAC system. Three validation test cases in laboratories have been demonstrated, yielding an overall satisfying cross-shore wave height, free surface set-up and set-down as well as the undertow, especially for the barred beach and a bathymetry composed of an irregular profile. For the test case of a constant slope, similar numerical settings produce a delayed wave breaking (to the offshore direction) compared to the measurements, as well as an underestimated undertow to an order of two. It could be related to the lacking of a roller, which stores partially the wave energy during breaking, and releases it gradually along with the wave propagation in the surf zone. The differences in model perfomances could also be attributed to the possible interference caused by the deactivation of the bottom friction laws in TELEMAC-2D for all laboratory cases listed in this study.

Another possibility is that to evaluate the Stokes drift for a spectrum, in our study, bulk parameters (such as the peak frequency wave number) have been used. It could also be evaluated for each component and then the total Stokes drift is the sum from the contribution of all components.

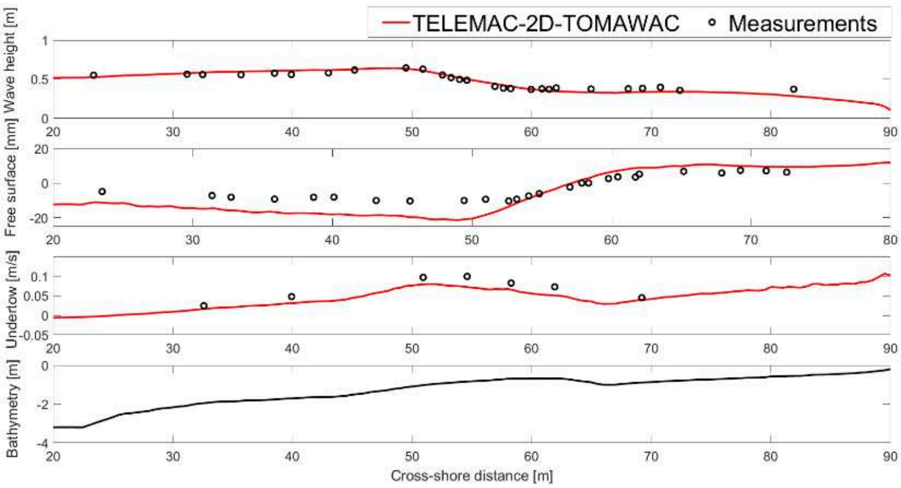

Figure 7 Simulate wave height, free surface and undertow have been compared to the measurements for the barred test case presented in [10].

ACKNOWLEDGEMENT

This work has been carried out in the framework of the CREST IWT-150028 project (www.crestproject.be)

REFERENCES

[1] Andrews, D.G, McIntyre, M.E. (1978), An exact theory of nonlinear waves on a Lagrangian-mean flow, Vol. 89, part 4, pp. 609-646

[2] Ardhuin, F, Rascle, N. Belibassakis, K. (2008), Explicit wave-averaged primitive equations using a Generalized Lagrangian mean, Vol. 20, Issue 1, pp. 35-60

[3] Bühler, O. (2014), Waves and mean flows (2nd edition), Cambridge University Press.

[4] Buhr Hansen. J, Svendsen I.A. (1984), A theoretical and experimental study of undertow, Proc. 19th Int. Conf. on Coastal Engineering, Houston: ASCE, pp 2246-2262.

[5] Prandle, D., Hargreaves, J.C., McManus, J.P., Campbell, A.R., Duwe, K., Lane, A., Mahnke, P., Shimwell, S., Wolf, J. (2000), Tide, wave and suspended sediment modelling on an open coast – Holderness, Coastal Engineering, Vol.41 , pp. 237-267.

[6] Garcez Faria, A.F.G., Thornton, E.B., Lippmann, T.C.,Stanton, T.P. (2000). Undertow over a barred beach, J. Geophys. Res., 105 (C7), 16999-1 7010

[7] Longuet-Higgins, M., Stewart, R. (1962), Radiation stress and mass transport in gravity waves, with application to surf beats. J. Fluid Mech., Vol. 13, pp 481-504

[8] Maria João Teles, Thierry Fouquet, Antonio Pires-Silva, Michel Benoit (2019), Computation of 3D coastal hydrodynamics through the vortex force formalism implemented by coupling TOMAWAC and TELEMAC-3D , Proceedings of the TELEMAC-User Conference 2019

[9] Okayasu, A., Shibayama, T., Horikawa, K. (1998), Vertical variation of undertow in surf zone. In Proceedings, 21st international Conference on Coastal Engineering, ASCE, 1998.

[10] Scott, C.P., Cox, D.T., Maddux, T. B., Long, J.W. (2005), Large-scale laboratory observations of turbulence on a fixed barred beach. Measurement Science and Technology 16, 1903–1912.

[11] Sultan, N.J. (1995), Irregular wave kinematics in the surf zone, Ph.D thesis, Texas A&M University (1995).

[12] Van den Bremer, T.S, Breivik, Ø (2018), Stokes drift, Philosophical Transactions. Series A, Mathematical, Physical, and Engineering Sciences, Vol. 376, pp. 2111.

Appendix Subroutine for computing Stokes drift:

```
            SUBROUTINE UVSTOKES_2D

    &  (UST, VST, FS,
    DEPTH,NPLAN,NF,NPOIN2,FREQ,DFREQ,TAILF,SCOSTE,SS
    INT)

    USE BIEF
    USE DECLARATIONS_TOMAWAC, ONLY: DEUPI
    USE INTERFACE_TOMAWAC

   IMPLICIT NONE

    INTEGER,INTENT(IN)            :: NPLAN,NF,NPOIN2
    DOUBLE PRECISION,INTENT(IN)   :: TAILF,
    SCOSTE(NPLAN)
    DOUBLE PRECISION,INTENT(IN)   ::
    FS(NPOIN2,NPLAN,NF)
    DOUBLE PRECISION,INTENT(IN)   :: DEPTH(NPOIN2)
    DOUBLE PRECISION,INTENT(IN)   ::
    FREQ(NF),DFREQ(NF)
    DOUBLE PRECISION,INTENT(IN)   :: SSINTE(NPLAN)
    DOUBLE PRECISION,INTENT(OUT)  :: UST(NPOIN2),
    VST(NPOIN2)

    DOUBLE PRECISION DTETAR, E(NPOIN2)
    DOUBLE PRECISION TAUX1(NPOIN2), TAUX2(NPOIN2)
    DOUBLE PRECISION TAUX3(NPOIN2), TAUX4(NPOIN2)
    DOUBLE PRECISION FP(NPOIN2)
    DOUBLE PRECISION SIGMA(NPOIN2)
    DOUBLE PRECISION XK(NPOIN2)
    DOUBLE PRECISION VARIAN(NPOIN2)
    DOUBLE PRECISION UV_STOKES(NPOIN2)
    DOUBLE PRECISION MEANDIR(NPOIN2)

    INTEGER  IPP
    DOUBLE PRECISION GAMMA_BREAKING

    DTETAR=DEUPI/DBLE(NPLAN)
    GAMMA_BREAKING= 0.4D0

    DO IPP=1,NPOIN2
       UST(IPP) = 0.D0
       VST(IPP) = 0.D0
    ENDDO

    ! COMPUTE PEAK FREQUENCY FOR ALL THE NODES IN 2D
    MESH
    CALL FREPIC(FP,FS,FREQ, NF, NPLAN ,
    NPOIN2,TAUX1,TAUX2)


    ! COMPUTE PEAK SIGMA AND K CORRESPONDING TO PEAK
    FREQUENCY
   DO IPP = 1,NPOIN2
      CALL WNSCOU(XK(IPP) ,FP(IPP) ,DEPTH(IPP))
   ENDDO

   ! COMPUTE TOTAL ENERGY/VARIANCE (UNIT: M2)
   CALL TOTNRJ
        &(VARIAN, FS, FREQ, DFREQ, TAILF,
        &  NF, NPLAN, NPOIN2)



   ! COMPUTE TOTAL STOKES DRIFT
   DO IPP = 1,NPOIN2
      SIGMA(IPP) = DEUPI*FP(IPP)
      IF (DEPTH(IPP) .GT. 0.01D0) THEN
           UV_STOKES(IPP) =
   SIGMA(IPP)*VARIAN(IPP)/DEPTH(IPP)/
     TANH(XK(IPP)*DEPTH(IPP))
         ELSE
           UV_STOKES(IPP) = 0.D0
     ENDIF
    ENDDO

   ! COMPUTE MEAN DIRECTION
         CALL TETMOY(MEANDIR,FS,SCOSTE,SSINTE,
        &
   NPLAN,FREQ,DFREQ,NF,NPOIN2,TAILF,TAUX1,
        &            TAUX2,TAUX3,TAUX4)


   DO IPP = 1,NPOIN2
      UST(IPP) = UV_STOKES(IPP)*SIN(MEANDIR(IPP))
      VST(IPP) = UV_STOKES(IPP)*COS(MEANDIR(IPP))
   ENDDO


   RETURN
   END
```